

CORVUS: Red-Teaming Hallucination Detectors via Internal Signal Camouflage in Large Language Models

Nay Myat Min¹, Long H. Pham¹, Hongyu Zhang², Jun Sun¹

¹Singapore Management University

²Chongqing University

Correspondence: myatmin.nay.2022@phdcs.smu.edu.sg

Abstract

Single-pass hallucination detectors rely on internal telemetry (e.g., uncertainty, hidden-state geometry, and attention) of large language models, implicitly assuming hallucinations leave separable traces in these signals. We study a white-box, model-side adversary that fine-tunes lightweight LoRA adapters on the model while keeping the detector fixed, and introduce CORVUS, an efficient red-teaming procedure that learns to camouflage detector-visible telemetry under teacher forcing, including an embedding-space FGSM attention stress test. Trained on 1,000 out-of-distribution Alpaca instructions (< 0.5% trainable parameters), CORVUS transfers to FAVA-Annotation across Llama-2, Vicuna, Llama-3, and Qwen2.5, and degrades both training-free detectors (e.g., LLM-Check) and probe-based detectors (e.g., SEP, ICR-probe), motivating adversary-aware auditing that incorporates external grounding or cross-model evidence.

1 Introduction

Large language models (LLMs) remain prone to hallucination—fluent but unfounded content that impairs reliability in QA, summarization, and open-ended generation (Ji et al., 2023; Zhang et al., 2025a; Huang et al., 2025). Broadly, hallucination defenses can be grouped into two categories: *external knowledge-based* approaches, which query external tools or corpora (e.g., retrieval) and judge an answer by its agreement with retrieved evidence, and *internal telemetry-based* approaches, which decide using only the model’s own computations. In this work, we focus on the latter class.

Within internal telemetry-based approaches, a growing line of work studies *single-pass* detectors: given a prompt and a realized answer, they use one teacher-forced forward pass to inspect token-level uncertainty and internal activations (such as hidden states, attentions). These methods implic-

itly assume hallucinations induce *separable telemetry* that can be read out from one pass. We consider both training-free scores (e.g., PPL (Ren et al., 2023), Window-Entropy (Malinin and Gales, 2021), LLM-Check (Sriramanan et al., 2024)) and probe-based detectors (e.g., SEP (Kosken et al., 2025), ICR-probe (Zhang et al., 2025b)).

Prior evaluations typically treat the LLM as *passive*: detectors may adapt to the model, but the model does not adapt in return. In open-weight or self-hosted deployments, a *white-box, model-side* adversary can modify the LLM (e.g., lightweight adapter finetuning) to *mask* detector-visible telemetry while keeping the surface answer unchanged. We therefore compare clean vs. adapted models under a *fixed-answer, teacher-forced replay* protocol (§5), so detector differences reflect internal changes rather than different generations.

We introduce *CORVUS* (Camouflaging Open-weight Representations, Volumes, Uncertainty, and Structure), a model-side red-teaming procedure that learns lightweight adapters to *camouflage the internal telemetry* used by single-pass detectors. CORVUS directly optimizes three general telemetry signals over answer tokens: (i) *hidden log-volume (HV)*, which summarizes how the answer-token representations spread out in hidden space; (ii) *attention diagonality (AD)*, which measures how self-focused attention is within the answer span; and (iii) *token entropy (TE)*, which captures how peaked the next-token distribution is. CORVUS uses a single-step Fast Gradient Sign Method (FGSM) (Goodfellow et al., 2015) in embedding space to construct a telemetry-directed *stress test* for attention diagonality: the perturbation is crafted to *increase* an attention-based detector score on the embeddings.

Contributions. We introduce CORVUS and evaluate single-pass hallucination detectors under a white-box, model-side adversary that efficiently adapts the model via lightweight adapters.

- **Method.** We define answer-window telemetry (TE/HV/AD) and train LoRA adapters under teacher forcing to reshape it, including a one-step embedding-space FGSM attention term.
- **OOD training.** We train CORVUS only on 1,000 out-of-distribution Alpaca instructions and never use FAVA-Annotation (Mishra et al., 2024) prompts for training; the same adapters transfer to FAVA without further tuning.
- **Evasion results.** On FAVA-Annotation across four open-weight LLMs (Llama-2, Vicuna, Llama-3, Qwen2.5), CORVUS degrades all the existing detectors calibrated on clean telemetry, including training-free scores (LLM-Check (Sriramanan et al., 2024)) and trained probes (ICR-probe (Zhang et al., 2025b), SEP (Kossen et al., 2025)).
- **Mechanism.** We connect controlled shifts in TE/HV/AD to failures of fixed detector scores, showing how modest adapter updates can collapse telemetry separability (§7).

Intuitively, single-pass telemetry-based detectors resemble exit polls: they infer outcomes from process traces rather than auditing external evidence. CORVUS is the strategic respondent—it adapts the model so that, for the same surface answer, detector-visible telemetry looks typical and becomes less distinguishable to a fixed detector.

2 Background: Hallucination Detection

Training-free defenses. Sampling-based approaches like SelfCheckGPT (Manakul et al., 2023) assess consistency across multiple generations but incur substantial latency. Single-pass uncertainty metrics such as per-token perplexity (Ren et al., 2023) and token-entropy-based scores (Malinin and Gales, 2021) are efficient but can be brittle to calibration and prompt shifts. Representation-centric methods summarize structure in attentions and hidden states (e.g., eigenvalue or log-determinant surrogates (Chen et al., 2024)); LLM-Check (Sriramanan et al., 2024) combines uncertainty with log-determinant features from hidden-state covariance (*Hidden Score*) and attention kernels (*Attention Score*) under teacher forcing.

Training-based defenses. Probe methods train lightweight classifiers over hidden states (Azaria and Mitchell, 2023; CH-Wang et al., 2024). Semantic Entropy Probes (SEP) (Kossen et al., 2025)

fit a small head on a selected hidden state to predict semantic-entropy-derived targets, enabling single-pass inference without sampling, but can be sensitive to dataset shift. ICR-probe (Zhang et al., 2025b) summarizes cross-layer residual-stream dynamics by comparing attention-guided attribution to actual hidden updates, then pools layerwise discrepancies with a small MLP.

Across these detectors, a shared premise holds: hallucinations leave *distinguishable telemetry* in the model’s computations, including uncertainty shifts, changes in hidden-state geometry, and attention structure (and, for ICR-probe, residual-attention mismatch). In our notation, these correspond to TE/HV/AD and related cross-layer signals. This shared premise motivates a model-side adversary that learns to camouflage such telemetry without materially altering the generated text.

Retrieval-augmented defenses. External knowledge based approaches, alignment scoring with external references (e.g., AlignScore (Zha et al., 2023)) and RAG-specific mechanisms (e.g., Re-DeEP (Sun et al., 2025)) can be strong when high-quality evidence exists, but they change the threat surface and may not apply to open-ended generation or settings where retrieval is unavailable.

3 The Proposed CORVUS Method

3.1 Method overview

CORVUS is a model-side red-teaming procedure that trains lightweight adapters to camouflage the telemetry used by single-pass hallucination detectors. With the detector fixed and the base model frozen, CORVUS optimizes only the adapters under the auditor’s teacher-forced replay on fixed (prompt, answer) pairs: a clean pass computes TE/HV/AD over the answer window, an AD-targeted FGSM embedding perturbation induces a stress-test pass, and a joint loss preserves teacher-forced likelihood while shifting telemetry. As the objective is label-free, adapters can be trained on an out-of-distribution dataset and still transfer to the audited dataset (see Figure 1 and Algorithm 1).

3.2 Threat model

We consider an adaptive, model-side adversary (red team) with white-box access to hidden states and attentions and the ability to fine-tune lightweight adapters. The goal is to reduce the hallucination confidence of a telemetry-based fixed detector under single-pass, teacher-forced auditing while pre-

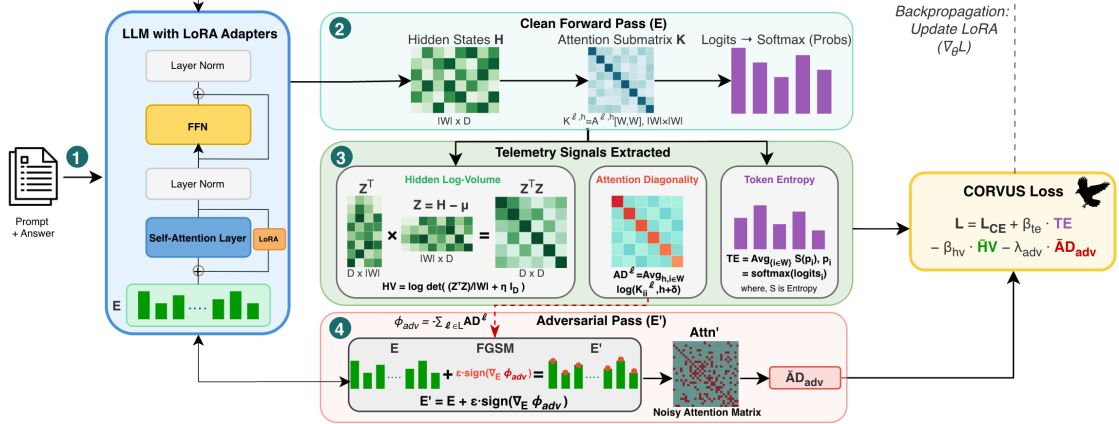


Figure 1: **CORVUS method.** (1) A prompt and fixed answer are processed under teacher forcing with trainable LoRA adapters. (2) A clean pass yields logits, hidden states, and attention over the answer window. (3) Telemetry features are extracted: TE, HV, and AD. (4) An AD-targeted single-step FGSM embedding perturbation induces a perturbed pass to obtain AD_{adv} ; a combined loss updates only LoRA to reshape detector-relevant internal signals.

serving task utility and, to the extent possible, the user-visible answer content. We focus on post-hoc auditing where an auditor evaluates a *realized* answer string via teacher-forced replay; correspondingly, our primary evaluation holds the answer string fixed when comparing clean vs. CORVUS-adapted models. This isolates internal-signal camouflage from textual changes. We realistically assume that the adversary has no hallucination-labeled examples from the target benchmark distribution, so CORVUS trains only on an out-of-distribution instruction set and optimizes telemetry terms that transfer to the auditing setting. We target a practical budget (single GPU) and do not rely on multiple generations or external retrieval.

3.3 Terminology

We consider decoder-only LLMs evaluated under *teacher forcing*. For an input sequence of T tokens, the model produces layerwise hidden states $\{X^\ell\}_{\ell=0}^L$ and attention probabilities $\{A^{\ell,h}\}_{\ell=1,h=1}^{L,H}$. Here $X^\ell \in \mathbb{R}^{T \times D}$ denotes hidden states at layer ℓ , where D is the model hidden size (with X^0 denoting input embeddings), and $A^{\ell,h} \in \mathbb{R}^{T \times T}$ denotes the head-wise attention distributions (after softmax) for head h at layer ℓ . When a single attention matrix is needed, we use the head-averaged attention $\text{Attn}^\ell = \frac{1}{H} \sum_{h=1}^H A^{\ell,h}$.

We focus on answer tokens in an *answer window* $W \subseteq \{0, \dots, T-1\}$. During CORVUS training on instruction-response pairs, the label mask identifies answer positions and we take W to be the set of non-ignore indices. For evaluation, we tokenize the prompt x_p (length p) and the answer string x to

form the concatenated sequence $x_p \oplus x$ with total length T , and set $W = \{p, p+1, \dots, T-1\}$, i.e., all tokens corresponding to the answer.

3.4 Telemetry over internal signals

We compute three general differentiable telemetry signals over W in one teacher-forced pass: token entropy (TE), hidden log-volume (HV), and attention diagonality (AD). TE captures token uncertainty, HV summarizes answer-token dispersion, and AD measures self-focused attention within the answer span; together they form a compact summary exploited by many detectors and CORVUS.

Token entropy (TE). Let $L \in \mathbb{R}^{T \times V}$ be teacher-forced logits over a vocabulary of size V , and let $p_i = \text{softmax}(L_i)$ denote the predictive distribution at token position i . We define *Token Entropy* (TE) as the mean token-level predictive entropy over the answer window W :

$$\text{TE} = \frac{1}{|W|} \sum_{i \in W} \left(- \sum_{v=1}^V p_i[v] \log p_i[v] \right). \quad (1)$$

TE is the mean categorical entropy of the next-token distribution over answer tokens (often known as logit entropy); windowed variants take a maximum to emphasize localized uncertainty spikes.

Hidden log-volume (HV). For each layer ℓ , let $X_W^\ell \in \mathbb{R}^{|W| \times D}$ be the slice of X^ℓ over answer tokens. We first center hidden states across tokens, $Z = X_W^\ell - 1\mu^\top$ with $\mu = \frac{1}{|W|} \sum_{i \in W} X_i^\ell \in \mathbb{R}^D$ (each $X_i^\ell \in \mathbb{R}^D$). We then form a feature-space

covariance proxy

$$C_{\text{hid}}^\ell = \frac{Z^\top Z}{|W|} + \eta I_D, \quad \eta > 0, \quad (2)$$

and define the HV as the log-determinant

$$HV^\ell = \log \det(C_{\text{hid}}^\ell). \quad (3)$$

We use a small jitter ($\eta = 10^{-3}$) for numerical stability and to handle the common case $|W| < D$ (rank-deficient covariance without regularization). This logdet-style proxy is the hidden-state regularizer used in our CORVUS implementation and is closely related to log-volume surrogates used by training-free detectors such as LLM-Check.

Attention diagonality (AD). For each layer ℓ and head h , let $K^{\ell,h} = A^{\ell,h}[W, W] \in \mathbb{R}^{|W| \times |W|}$ denote the attention submatrix restricted to answer tokens. We summarize diagonal concentration by

$$AD^\ell = \frac{1}{H} \sum_{h=1}^H \left[\frac{1}{|W|} \sum_{i \in W} \log(K_{ii}^{\ell,h} + \delta) \right], \quad \delta > 0. \quad (4)$$

We use $\delta = 10^{-8}$ for numerical stability to avoid $\log 0$ from (near-)zero diagonal attention probabilities. Higher AD^ℓ corresponds to more self-diagonal attention mass, and averaging across layers yields a scalar closely related to the diagonal component of LLM-Check’s Attention Score.

3.5 Detector assumptions and signals

We briefly summarize the primary signals used by representative single-pass detectors and how they relate to TE/HV/AD:

- **PPL** (Ren et al., 2023): a sequence-level proxy of output uncertainty derived from per-token negative log-likelihood of the token, closely tied to TE over the answer window.
- **Window-Entropy** (Malinin and Gales, 2021): an entropy-based uncertainty score over the answer window. We use a windowed token-entropy variant and take the maximum over windows, which reduces to the maximum token entropy over the answer window.
- **LLM-Check** (Sriramanan et al., 2024): a training-free detector that aggregates output-uncertainty features with representation-centric features. In our notation, its Hidden Score is a global log-volume surrogate closely related to HV (a mean log-determinant / log-spectrum of a hidden-state covariance proxy),

and its Attention Score corresponds to a global variant of AD (mean log of attention diagonal mass), both computed under teacher forcing.

- **SEP** (Kosken et al., 2025; Kuhn et al., 2023): a probe trained to predict semantic-entropy-derived targets from a single hidden state, coupling TE-like uncertainty with representation information at a chosen layer.
- **ICR-probe** (Zhang et al., 2025b): a probe over *cross-layer* residual-stream dynamics that compares attention-guided attribution to actual hidden-state updates and pools these discrepancies across layers with a small MLP.

Observation. On clean models evaluated on FAVA-Annotation, TE/HV/AD exhibit consistent distribution shifts between faithful and hallucinated answers, and these shifts are exploitable by single-pass detectors. CORVUS targets this vulnerability by inducing internal-signal shifts so that clean-calibrated decision rules (e.g., fixed thresholds) do not transfer, and in some cases the telemetry becomes less distinguishable.

3.6 Adversarial embedding red-teaming

FGSM is used as a telemetry-directed surrogate: we craft a one-step embedding perturbation to *increase* an attention-based detector score proportional to low attention diagonality (i.e., to *decrease* AD). This does not imply the perturbed pass induces semantic hallucinations or incorrect answers. Concretely, we apply a single-step perturbation in embedding space and then include a loss term that encourages higher AD on the perturbed pass. Let E denote the input embeddings for a batch of tokenized sequences. We define the FGSM objective on a forward pass with differentiable embeddings as

$$\phi_{\text{adv}} = - \sum_{\ell \in \mathcal{L}} AD^\ell, \quad (5)$$

and compute its gradient with respect to E . An FGSM update constructs perturbed embeddings

$$E' = E + \varepsilon \text{sign}(\nabla_E \phi_{\text{adv}}), \quad \varepsilon > 0, \quad (6)$$

which *increase* ϕ_{adv} and thus *decrease* attention diagonality. We then run a forward pass with E' (keep model parameters shared) and compute attention telemetry $\{AD_{\text{adv}}^\ell\}$ under this perturbation.

Algorithm 1 CORVUS training

Require: Model M ; tokenizer \mathcal{T} ; train data \mathcal{D} ; steps S_{\max}
Require: LoRA modules \mathcal{O} (rank r , scaling α); penalties $(\beta_{\text{te}}, \beta_{\text{hv}})$; FGSM step size ε ; λ_{adv} ; telemetry options (e.g., layer set \mathcal{L})

- 1: Attach LoRA($M, \mathcal{O}, r, \alpha$); freeze base parameters
- 2: **for** $s = 1$ to S_{\max} **do**
- 3: Sample (prompt, answer) $\sim \mathcal{D}$; tokenize with \mathcal{T} to obtain targets y , window W , and embeddings E
- 4: **Clean pass:** run M under teacher forcing; collect logits, hidden states, and attentions
- 5: $\text{TE}_{\text{clean}} \leftarrow \text{TOKENENTROPY}(W, \text{logits})$
- 6: $(\overline{\text{HV}}_{\text{clean}}, \overline{\text{AD}}_{\text{clean}}) \leftarrow \text{TELEMETRY}(W, \text{hidden}, \text{attn}, \mathcal{L})$
- 7: $\phi_{\text{adv}} \leftarrow -\sum_{\ell \in \mathcal{L}} \text{AD}^{\ell}$ // detector score proxy
- 8: $E' \leftarrow E + \varepsilon \text{ sign}(\nabla_E \phi_{\text{adv}})$ // FGSM
- 9: **Adversarial pass:** run M with E' ; collect attn'
- 10: $\overline{\text{AD}}_{\text{adv}} \leftarrow \text{TELEMETRY}(W, \cdot, \text{attn}', \mathcal{L})$ // AD only
- 11: $\mathcal{L}_{\text{CE}} \leftarrow \text{CE_LOSS}(\text{logits}, y)$
- 12: $\mathcal{L} \leftarrow \mathcal{L}_{\text{CE}} + \beta_{\text{te}} \text{TE}_{\text{clean}}$
 $\quad - \beta_{\text{hv}} \overline{\text{HV}}_{\text{clean}} - \lambda_{\text{adv}} \overline{\text{AD}}_{\text{adv}}$
- 13: Backpropagate $\nabla_{\theta_{\text{LoRA}}} \mathcal{L}$; update LoRA parameters
- 14: **end for**

3.7 Training objective

Figure 1 provides an overview of the CORVUS training procedure and Algorithm 1 summarizes the full training loop. Let (\cdot) denote layerwise means on the clean or adversarial forward (e.g., $\overline{\text{HV}}_{\text{clean}} = \frac{1}{|\mathcal{L}|} \sum_{\ell \in \mathcal{L}} \text{HV}^{\ell}$ over a set of monitored layers \mathcal{L}). For a given batch, the CORVUS loss is

$$\mathcal{L} = \mathcal{L}_{\text{CE}} + \beta_{\text{te}} \text{TE}_{\text{clean}} \quad (7)$$

$$\quad - \beta_{\text{hv}} \overline{\text{HV}}_{\text{clean}} - \lambda_{\text{adv}} \overline{\text{AD}}_{\text{adv}}.$$

where \mathcal{L}_{CE} is the standard sequence-level cross-entropy loss under teacher forcing, and $\beta_{\text{te}}, \beta_{\text{hv}}, \lambda_{\text{adv}} > 0$ are scalar coefficients. The TE term penalizes token entropy on the clean pass, the HV term is maximized to adversarially shift hidden-geometry features, and the adversarial AD term $-\lambda_{\text{adv}} \overline{\text{AD}}_{\text{adv}}$ encourages higher diagonality on the perturbed pass. The FGSM direction is computed by differentiating the surrogate detector score $-\overline{\text{AD}}$ with respect to the input embeddings. All telemetry terms are computed under teacher forcing over the answer window, matching the detector feature-extraction protocol.

4 Training and Implementation Details

Telemetry computation. We compute token-level *TE* and per-layer *HV* and *AD* on the answer tokens (as defined by the label mask / answer window), following §3.4. We average *HV/AD* across a monitored layer set \mathcal{L} on-the-fly. For the adversarial term, gradients flow through the adversarial pass (via $\overline{\text{AD}}_{\text{adv}}$) into LoRA parameters; clean

telemetry values are used as loss terms but are not explicitly matched between passes.

Adapter fine-tuning. CORVUS uses lightweight adapter-based fine-tuning to preserve base model capacity while optimizing the evasion objective. In our runs (implemented via LLaMA-Factory (Zheng et al., 2024)), we attach LoRA adapters with rank $r=64$ and scaling $\alpha=128$, and target only the attention projection modules ($q_{\text{proj}}, k_{\text{proj}}$). All base model parameters are frozen. Training uses bfloat16, gradient accumulation (4 steps), gradient checkpointing, and AdamW with learning rate 2×10^{-4} and a cosine learning-rate scheduler.

Objective weighting. The loss uses penalties $(\beta_{\text{te}}, \beta_{\text{hv}})$ and λ_{adv} (Eq. 7). HV enters with a negative sign to increase hidden log-volume along the monitored layer band; TE enters with a positive sign to penalize high token entropy over response tokens; and the adversarial attention term enters with a negative sign on $\overline{\text{AD}}_{\text{adv}}$, which increases attention diagonality on the perturbed pass over the same layer band. Our default coefficients are: $\beta_{\text{te}} = 0.07$, $\beta_{\text{hv}} = 0.05$, and $\lambda_{\text{adv}} = 0.5$.

Adversarial step. We apply FGSM with magnitude $\varepsilon=1.0 \times 10^{-2}$ at each update. We first run an embedding-gradient pass to compute $\nabla_E \phi_{\text{adv}}$, and then run a second pass with perturbed embeddings to compute the adversarial *AD* term (Eq. 7). The perturbed embeddings are not clamped or projected back to the original embedding manifold.

Data and batching. We train CORVUS adapters on the Alpaca_en dataset (Taori et al., 2023) via LLaMA-Factory. This corpus is *out-of-distribution* relative to FAVA-Annotation: it consists of generic instruction-response pairs without hallucination labels, and we do not use any FAVA-Annotation prompts or labels when optimizing the CORVUS objective. The base loss is standard sequence-level cross-entropy under teacher forcing; the label mask defines the answer tokens for TE/HV/AD.

Compute and measurement. Experiments run on a single GPU node (H100), 8 CPU cores, and 48 GB system RAM. We train for a single epoch over the 1,000 Alpaca examples with cosine learning-rate scheduling. The resulting adapters are then evaluated zero-shot on FAVA-Annotation. We next describe the detectors, benchmark, and fixed-answer replay protocol used to evaluate CORVUS.

5 Evaluation Setup

5.1 Detectors and Baselines

We evaluate CORVUS against two families of state-of-the-art single-pass detectors under a teacher-forced replay on fixed (prompt, answer) pairs:

- **Training-free detectors.** We consider standard single-pass uncertainty and representation-centric scores: PPL, Window-Entropy (max token entropy over the answer window; $w=1$), and LLM-Check (Hidden/Attention Scores).
- **Training-based detectors.** We also consider SEP (single-state probe) and ICR-probe (MLP over layerwise residual–attention mismatch). Probes are trained on clean-model telemetry (FAVA-train) and tested on held-out examples.

5.2 Benchmark and Models

We ground our evaluation in the FAVA-Annotation dataset introduced by (Mishra et al., 2024), which consists of prompts and model-generated answers annotated with sequence-level hallucination labels. We follow the split protocol from LLM-Check for training, validation, and test partitions. We experiment with four open-weight, instruction-tuned LLMs commonly used in hallucination-detection work: Llama-2-7B-Chat (Touvron et al., 2023), Vicuna-7B (Zheng et al., 2023), Llama-3-8B-Instruct (Grattafiori et al., 2024), and Qwen-2.5-14B-Instruct (Qwen et al., 2025). For each model, we associate each FAVA-Annotation prompt with a benchmark-provided answer string.

5.3 Protocol

For each model, we compare a clean base model (no adapters) to a CORVUS-adapted model (LoRA fine-tuned on Alpaca). All detectors are computed via teacher-forced replay on a given (prompt, answer) pair. We use a *fixed-answer replay* protocol: for each prompt, we reuse the benchmark-provided answer string when extracting telemetry from both models. Importantly, it is also a conservative restriction for an attacker: allowing benign rephrasing or changing the answer distribution can only make evasion easier, whereas our goal is to show that detector reliability can fail due to internal-signal shifts even when the surface text is held constant. Training-based detectors (SEP, ICR-probe) are *trained only* on clean-model telemetry from the FAVA-Annotation training split and then evaluated

unchanged on both clean and CORVUS telemetry (auditor fixed; model changes). CORVUS adapters are trained only on Alpaca, so performance on FAVA reflects out-of-distribution transfer.

Evaluation metrics. For each detector and model on FAVA-Annotation, we report: *AUROC*, as a threshold-independent measure of hallucination detection performance, *Accuracy* and *F1* at an operating point chosen on the validation set; and *Fixed-threshold deltas*: calibrate a threshold on the clean model at a target false-positive rate (e.g., 5% FPR) and evaluate the same threshold under CORVUS, reporting changes in accuracy, FPR, TPR, and AUROC. We do not require the CORVUS-adapted model to reproduce the same answer under free decoding; generation-time changes are orthogonal to the post-hoc auditing we target.

Utility preservation sanity check. Although CORVUS is trained to reshape telemetry under teacher forcing (and is not optimized to preserve free-decoding generations), we verify that the learned adapters do not induce a trivial generation failure mode under free decoding. In a representative run (500 prompts, greedy), both the base and CORVUS-adapted models produced *non-empty* responses with *no refusal-style outputs*, and we did not observe repetition collapse (95th-percentile maximum consecutive word-run of 2). This indicates that detector evasion is not explained by a degenerate “non-generating” or “refusal-only” collapse, and that the adapted model retains generation utility (readable, instruction-following outputs). As a lightweight surface-form fluency proxy, we also compute external-LM perplexity (GPT-2 (Radford et al., 2019)) on the answers; the median perplexity shifts modestly from 11.1 (base) to 13.7 (ours).

6 Results

We evaluate CORVUS on *FAVA-Annotation* with four open-weight LLMs. Table 1 compares *clean* vs. *CORVUS-adapted* models under identical prompts and fixed-answer teacher-forced replay. For each detector/model pair, we report AUROC, accuracy, TPR at a fixed FPR, F1, and the change induced by attaching CORVUS adapters. Across all four models on FAVA-Annotation, CORVUS reduces the effectiveness of both training-free and training-based detectors. Training-free scores (PPL, Window-Entropy, and LLM-Check and its components) and trained probes (SEP and ICR-

Metric	AUROC	Accuracy	TPR@5%FPR	F1
Llama-2-7B-Chat				
PPL Score	53.18 → 48.09 (-5.10)	58.68 → 50.90 (-7.78)	3.59 → 0.00 (-3.59)	68.92 → 5.75 (-63.17)
Window-Entropy	56.99 → 55.30 (-1.69)	57.19 → 48.50 (-8.69)	7.19 → 1.20 (-5.99)	42.11 → 2.27 (-39.84)
Hidden (L17)	58.15 → 54.10 (-4.04)	56.89 → 50.00 (-6.89)	8.98 → 0.00 (-8.98)	64.36 → 0.00 (-64.36)
Attn Score (L20)	73.63 → 48.08 (-25.54)	69.76 → 50.00 (-19.76)	10.18 → 0.00 (-10.18)	69.85 → 0.00 (-69.85)
SEP	61.79 → 44.89 (-16.90)	52.36 → 50.00 (-2.36)	4.05 → 3.38 (-0.67)	66.51 → 6.67 (-59.84)
ICR Probe	71.44 → 52.36 (-19.08)	71.74 → 34.78 (-36.96)	98.31 → 30.77 (-67.54)	81.69 → 40.00 (-41.69)
Vicuna-7B (v1.5)				
PPL Score	54.07 → 50.40 (-3.67)	49.40 → 36.30 (-13.10)	3.59 → 0.00 (-3.59)	6.63 → 0.00 (-6.63)
Window-Entropy	45.43 → 47.10 (+1.67)	48.50 → 35.70 (-12.80)	0.60 → 1.40 (+0.80)	1.15 → 2.63 (+1.48)
Hidden (L13)	58.19 → 58.00 (-0.19)	52.40 → 36.30 (-16.10)	9.58 → 0.00 (-9.58)	16.75 → 0.00 (-16.75)
Attn Score (L18)	71.91 → 59.70 (-12.21)	60.78 → 36.30 (-24.48)	25.75 → 0.00 (-25.75)	39.63 → 0.00 (-39.63)
SEP	67.63 → 44.78 (-22.85)	54.05 → 50.34 (-3.72)	11.49 → 2.03 (-9.46)	41.38 → 3.92 (-37.46)
ICR Probe	69.70 → 62.00 (-7.70)	67.39 → 35.90 (-31.49)	18.50 → 0.10 (-18.40)	79.45 → 36.20 (-43.25)
Llama-3-8B-Instruct				
PPL Score	53.22 → 50.00 (-3.22)	58.68 → 36.30 (-22.38)	3.59 → 0.00 (-3.59)	67.40 → 0.00 (-67.40)
Window-Entropy	60.17 → 62.10 (+1.93)	56.59 → 36.10 (-20.49)	2.99 → 0.30 (-2.69)	55.52 → 0.60 (-54.92)
Hidden (L21)	57.10 → 57.00 (-0.01)	51.80 → 36.30 (-15.50)	7.78 → 0.00 (-7.78)	14.24 → 0.00 (-14.24)
Attn Score (L22)	68.95 → 58.50 (-10.45)	53.89 → 36.30 (-17.59)	12.57 → 0.00 (-12.57)	21.89 → 0.00 (-21.89)
SEP	68.31 → 41.21 (-27.10)	57.09 → 47.30 (-9.80)	5.41 → 3.38 (-2.03)	56.36 → 7.14 (-49.21)
ICR Probe	72.78 → 53.00 (-19.78)	69.57 → 35.00 (-34.57)	25.75 → 8.00 (-17.75)	79.10 → 39.00 (-40.10)
Qwen2.5-14B-Instruct				
PPL Score	53.30 → 49.80 (-3.50)	49.10 → 35.90 (-13.20)	1.80 → 0.00 (-1.80)	3.41 → 0.00 (-3.41)
Window-Entropy	60.87 → 60.20 (-0.67)	52.40 → 41.20 (-11.20)	8.98 → 0.00 (-8.98)	15.87 → 0.00 (-15.87)
Hidden (L33)	60.44 → 58.88 (-1.56)	51.50 → 36.30 (-15.20)	7.19 → 0.00 (-7.19)	12.90 → 0.00 (-12.90)
Attn Score (L37)	68.06 → 46.50 (-21.56)	53.89 → 36.30 (-17.59)	11.98 → 0.00 (-11.98)	20.62 → 0.00 (-20.62)
SEP	68.90 → 46.20 (-22.70)	56.80 → 35.90 (-20.90)	9.00 → 0.00 (-9.00)	58.50 → 0.00 (-58.50)
ICR Probe	77.14 → 60.00 (-17.14)	66.80 → 36.30 (-30.50)	16.00 → 0.00 (-16.00)	70.00 → 42.16 (-27.84)

Table 1: **Results.** Values are Clean → After (Δ). Positive deltas (blue) indicate improved detection; negative (red) indicate successful evasion. *Hidden* and *Attn Scores* denote the corresponding components from LLM-CHECK.

probe) degrade when applied to CORVUS-adapted telemetry, despite probes being trained only on clean-model traces. We also report fixed-threshold deltas (clean-calibrated at 5% FPR) for entropy, attention, and hidden components. Thresholds are chosen on clean-model validation telemetry and then held fixed under CORVUS. Clean-calibrated thresholds can yield much higher FPR and lower TPR after adaptation, indicating brittleness to model-side attacks. Across models, clean-calibrated operating points often collapse (TPR@5%FPR near 0 and F1 near 0), revealing substantial calibration drift under model-side adaptation. Attention/representation-centric signals are the most brittle: the LLM-Check Attention Score loses up to 25.5 AUROC points (73.6→48.1 on Llama-2), and SEP/ICR-probe drop by 17–27 and up to 20 AUROC points, respectively.

Calibration shift vs. separability. To distinguish calibration shift from separability loss, we report both AUROC and fixed-threshold metrics. Large fixed-threshold drops with smaller AUROC

changes suggest calibration shift (clean-calibrated thresholds no longer transfer), while AUROC drops indicate reduced separability. We observe both effects across telemetry families. Additional ablations are reported in the Appendix B.

7 Mechanistic View of CORVUS

To interpret the degradations in Table 1, we provide a mechanistic view of why internal telemetry is, in general, not a reliable signal for hallucination detection under adaptive model-side attacks.

Detectors as functionals of telemetry. Let $T(x) \in \mathbb{R}^m$ denote single-pass, layer-aggregated telemetry features (e.g., token entropy, hidden-state geometry, attention structure, cross-layer residual-attention mismatch) computed on an input–output pair x , and let $s(x) = g(T(x))$ be the detector score. Training-free methods use a fixed aggregation $g(\cdot)$, while probe-based methods learn a shallow $g(\cdot)$ (e.g., MLP) on top of $T(x)$. Detection succeeds when the between-class separation $\Delta \triangleq \|\mathbb{E}_{x \in \mathcal{H}}[T(x)] - \mathbb{E}_{x \in \mathcal{F}}[T(x)]\|$ is large,

Detector	Telemetry read	CORVUS-affected telemetry
PPL	Per-token log-likelihood / PPL over answer window	TE term directly alters the token-level predictive distribution (and hence entropy/perplexity) under teacher forcing on the answer window.
Window-Entropy	Windowed token entropy over the answer window (max over windows)	Driven by entropy: CORVUS changes the token-level predictive distribution under teacher forcing (hence entropy statistics), while shifts in HV/AD that change routing can indirectly modify these distributions.
LLM-Check	Hidden log-det (<i>Hidden Score</i>); attention-kernel log-det (<i>Attention Score</i>)	HV term reshapes hidden log-volume features that feed the Hidden Score; AD term shapes diagonal attention patterns (and thus the attention log-det component).
SEP	Single-state probe predicting semantic-entropy-derived uncertainty	TE term changes uncertainty-related behavior of the model; HV and AD terms change the hidden representation at the probed layer from which SEP reads out, affecting the features the probe relies on.
ICR-probe	Layerwise JSD between residual-induced projection distributions and attention	AD influences the structure and concentration of attention distributions in the JSD; HV changes the hidden directions along which residual updates are measured, altering the projection-induced distributions.

Table 2: **Telemetry map.** Summary of which telemetry features different detectors primarily rely on and which components of the CORVUS objective interact with those features.

where \mathcal{H} and \mathcal{F} denote hallucinated and faithful instances, respectively. Empirically, on clean models and FAVA-Annotation, we observe such separability for TE, HV, and AD when used as part of LLM-Check-style features and probes.

How CORVUS changes telemetry. CORVUS modifies the model, not the detector: it fine-tunes lightweight adapters so that, under the same teacher-forced protocol, the induced telemetry $T(x)$ for hallucinated and faithful instances becomes less separable. The loss directly interacts with three components of $T(x)$: (i) the clean-pass token entropy over the answer window, TE_{clean} ; (ii) a clean-pass hidden log-volume term, HV_{clean} , that summarizes answer-window hidden Gram matrices across selected layers; and (iii) an adversarial attention-diagonal term, $\overline{\text{AD}}_{\text{adv}}$, computed after a single-step FGSM perturbation in embedding space. By penalizing TE_{clean} and shaping HV_{clean} and $\overline{\text{AD}}_{\text{adv}}$, CORVUS shifts the telemetry distribution that detectors read—without modifying the detector architecture or its training data. Consequently, the effective separation Δ shrinks and the score $s(x) = g(T(x))$ becomes less informative about hallucination labels, even when the surface answer is held fixed. Table 2 summarizes which telemetry components different detectors primarily read and which parts of the CORVUS affect them.

Why this does not reduce to “making the model dull.” A trivial evasion strategy would be to degrade the model (e.g., collapse activations or saturate logits), which harms task utility and is easily detectable. CORVUS avoids this by (i) retaining the standard teacher-forced cross-entropy loss, (ii) using small telemetry coefficients so LoRA updates

remain low-rank and low-magnitude, and (iii) applying the adversarial term via a one-step embedding perturbation rather than enforcing extreme attention patterns on clean inputs. We report a utility preservation sanity check in §5 to confirm the adapters do not trivially break generation.

Implications. Our results indicate that detectors should be evaluated not only on static, clean models but also under adaptive, model-side adversaries that can reshape internal telemetry. Robust defenses will likely require (i) diversity in telemetry signals that are harder to jointly manipulate with lightweight adapters, (ii) some form of randomization or challenge-response that makes white-box minimization more difficult, and (iii) cross-model validation (e.g., frozen auditors) to reduce the impact of on-model representation-level evasion.

8 Conclusion

We introduced CORVUS, a lightweight LoRA red-teaming method that camouflages single-pass telemetry (TE/HV/AD, with FGSM) under teacher-forced replay. Trained on 1,000 out-of-distribution Alpaca examples without detector labels, CORVUS transfers to FAVA-Annotation and degrades training-free scores (e.g., LLM-Check) and probe-based detectors (e.g., SEP, ICR-probe) across multiple open-weight models. Our results suggest that internal telemetry alone is not reliable for hallucination detection under adaptive model-side attacks, implying that external knowledge-based approaches, while challenging, may be inevitable for robust auditing. The open-source implementation of CORVUS is available at this [URL](#).

Limitations

CORVUS assumes white-box access to the LLM and is most applicable to open-source or self-hosted models where an adversary can extract representations and fine-tune lightweight adapters; it does not directly apply to closed APIs, except via surrogate-model attacks. Our evaluation is limited to single-pass detectors operating on one model’s internals; more advanced defenses (e.g., retrieval-based fact-checking) were out of scope and may counter this attack. Finally, CORVUS targets the model’s internals, not its factuality: we do not optimize for correctness, and the attack can hide a hallucination without fixing it. Developing attacks that improve factuality, or defenses that explicitly monitor factual consistency, are left for future work.

Ethical Considerations

This research is a form of adversarial red-teaming aimed at improving LLM safety. We demonstrate how an aligned LLM’s internal traces can be manipulated to evade hallucination detectors in a controlled setting. Our intent is to expose this vulnerability so that detector designers can patch it, not to facilitate misuse. We release our code in a responsible manner. All experiments were conducted on public datasets (Alpaca and FAVA-Annotation datasets) in accordance with their licenses. No private or user data was used. We strongly discourage any malicious use of CORVUS to bypass real-world safety systems. Instead, we hope this work informs the development of more robust hallucination defenses. For example, by incorporating adversarial training or cross-checks, ultimately leading to safer and more trustworthy AI systems.

References

Amos Azaria and Tom Mitchell. 2023. [The internal state of an LLM knows when it’s lying](#). In *Findings of the Association for Computational Linguistics: EMNLP 2023*, pages 967–976, Singapore. Association for Computational Linguistics.

Sky CH-Wang, Benjamin Van Durme, Jason Eisner, and Chris Kedzie. 2024. [Do androids know they’re only dreaming of electric sheep?](#) In *Findings of the Association for Computational Linguistics: ACL 2024*, pages 4401–4420, Bangkok, Thailand. Association for Computational Linguistics.

Chao Chen, Kai Liu, Ze Chen, Yi Gu, Yue Wu, Mingyuan Tao, Zhihang Fu, and Jieping Ye. 2024. [INSIDE: LLMs’ internal states retain the power of hallucination detection](#). In *The Twelfth International Conference on Learning Representations*.

Ian J. Goodfellow, Jonathon Shlens, and Christian Szegedy. 2015. [Explaining and harnessing adversarial examples](#). *Preprint*, arXiv:1412.6572.

Aaron Grattafiori, Abhimanyu Dubey, Abhinav Jauhri, Abhinav Pandey, Abhishek Kadian, Ahmad Al-Dahle, Aiesha Letman, Akhil Mathur, Alan Schelten, Alex Vaughan, Amy Yang, Angela Fan, Anirudh Goyal, Anthony Hartshorn, Aobo Yang, Archi Mitra, Archie Sravankumar, Artem Korenev, Arthur Hinsvark, and 542 others. 2024. [The llama 3 herd of models](#). *Preprint*, arXiv:2407.21783.

Lei Huang, Weijiang Yu, Weitao Ma, Weihong Zhong, Zhangyin Feng, Haotian Wang, Qianglong Chen, Weihua Peng, Xiaocheng Feng, Bing Qin, and Ting Liu. 2025. [A survey on hallucination in large language models: Principles, taxonomy, challenges, and open questions](#). *ACM Trans. Inf. Syst.*, 43(2).

Ziwei Ji, Nayeon Lee, Rita Frieske, Tiezheng Yu, Dan Su, Yan Xu, Etsuko Ishii, Ye Jin Bang, Andrea Madotto, and Pascale Fung. 2023. [Survey of hallucination in natural language generation](#). *ACM Comput. Surv.*, 55(12).

Jannik Kossen, Jiatong Han, Muhammed Razzak, Lisa Schut, Shreshth A Malik, and Yarin Gal. 2025. [Semantic entropy probes: Robust and cheap hallucination detection in LLMs](#).

Lorenz Kuhn, Yarin Gal, and Sebastian Farquhar. 2023. [Semantic uncertainty: Linguistic invariances for uncertainty estimation in natural language generation](#). *arXiv preprint arXiv:2302.09664*.

Andrey Malinin and Mark Gales. 2021. [Uncertainty estimation in autoregressive structured prediction](#). *Preprint*, arXiv:2002.07650.

Potsawee Manakul, Adian Liusie, and Mark Gales. 2023. [SelfCheckGPT: Zero-resource black-box hallucination detection for generative large language models](#). In *Proceedings of the 2023 Conference on Empirical Methods in Natural Language Processing*, pages 9004–9017, Singapore. Association for Computational Linguistics.

Abhika Mishra, Akari Asai, Vidhisha Balachandran, Yizhong Wang, Graham Neubig, Yulia Tsvetkov, and Hannaneh Hajishirzi. 2024. [Fine-grained hallucinations detections](#). *arXiv preprint*.

Qwen, :, An Yang, Baosong Yang, Beichen Zhang, Binyuan Hui, Bo Zheng, Bowen Yu, Chengyuan Li, Dayiheng Liu, Fei Huang, Haoran Wei, Huan Lin, Jian Yang, Jianhong Tu, Jianwei Zhang, Jianxin Yang, Jiaxi Yang, Jingren Zhou, and 25 others. 2025. [Qwen2.5 technical report](#). *Preprint*, arXiv:2412.15115.

Alec Radford, Jeff Wu, Rewon Child, David Luan, Dario Amodei, and Ilya Sutskever. 2019. [Language models are unsupervised multitask learners](#). *arXiv*.

Jie Ren, Jiaming Luo, Yao Zhao, Kundan Krishna, Mohammad Saleh, Balaji Lakshminarayanan, and Peter J Liu. 2023. [Out-of-distribution detection and selective generation for conditional language models](#). In *The Eleventh International Conference on Learning Representations*.

Gaurang Sriramanan, Siddhant Bharti, Vinu Sankar Sadasivan, Shoumik Saha, Priyatham Kattakinda, and Soheil Feizi. 2024. [LLM-Check: Investigating Detection of Hallucinations in Large Language Models](#). In *Advances in Neural Information Processing Systems*, volume 37, pages 34188–34216. Curran Associates, Inc.

ZhongXiang Sun, Xiaoxue Zang, Kai Zheng, Jun Xu, Xiao Zhang, Weijie Yu, Yang Song, and Han Li. 2025. [RedeEP: Detecting hallucination in retrieval-augmented generation via mechanistic interpretability](#). In *The Thirteenth International Conference on Learning Representations*.

Rohan Taori, Ishaan Gulrajani, Tianyi Zhang, Yann Dubois, Xuechen Li, Carlos Guestrin, Percy Liang, and Tatsunori B. Hashimoto. 2023. [Stanford alpaca: An instruction-following llama model](#). https://github.com/tatsu-lab/stanford_alpaca.

Hugo Touvron, Louis Martin, Kevin Stone, Peter Albert, Amjad Almahairi, Yasmine Babaei, Nikolay Bashlykov, Soumya Batra, Prajjwal Bhargava, Shruti Bhosale, Dan Bikel, Lukas Blecher, Cristian Canton Ferrer, Moya Chen, Guillem Cucurull, David Esiobu, Jude Fernandes, Jeremy Fu, Wenyin Fu, and 49 others. 2023. [Llama 2: Open foundation and fine-tuned chat models](#). *Preprint*, arXiv:2307.09288.

Yuheng Zha, Yichi Yang, Ruichen Li, and Zhiting Hu. 2023. [AlignScore: Evaluating factual consistency with a unified alignment function](#). In *Proceedings of the 61st Annual Meeting of the Association for Computational Linguistics (Volume 1: Long Papers)*, pages 11328–11348, Toronto, Canada. Association for Computational Linguistics.

Yue Zhang, Yafu Li, Leyang Cui, Deng Cai, Lemao Liu, Tingchen Fu, Xiting Huang, Enbo Zhao, Yu Zhang, Yulong Chen, Longyue Wang, Anh Tuan Luu, Wei Bi, Freda Shi, and Shuming Shi. 2025a. [Siren’s song in the ai ocean: A survey on hallucination in large language models](#). *Computational Linguistics*, pages 1–46.

Zhenliang Zhang, Xinyu Hu, Huixuan Zhang, Junzhe Zhang, and Xiaojun Wan. 2025b. [ICR probe: Tracking hidden state dynamics for reliable hallucination detection in LLMs](#). In *Proceedings of the 63rd Annual Meeting of the Association for Computational Linguistics (Volume 1: Long Papers)*, pages 17986–18002, Vienna, Austria. Association for Computational Linguistics.

Lianmin Zheng, Wei-Lin Chiang, Ying Sheng, Siyuan Zhuang, Zhanghao Wu, Yonghao Zhuang, Zi Lin, Zhuohan Li, Dacheng Li, Eric. P Xing, Hao Zhang, Joseph E. Gonzalez, and Ion Stoica. 2023. [Judging llm-as-a-judge with mt-bench and chatbot arena](#). *Preprint*, arXiv:2306.05685.

Yaowei Zheng, Richong Zhang, Junhao Zhang, Yanhan Ye, Zheyen Luo, Zhangchi Feng, and Yongqiang Ma. 2024. [Llamafactory: Unified efficient fine-tuning of 100+ language models](#). In *Proceedings of the 62nd Annual Meeting of the Association for Computational Linguistics (Volume 3: System Demonstrations)*, Bangkok, Thailand. Association for Computational Linguistics.

A Appendix

A.1 Acknowledgment of LLM Usage

We used AI-assisted tools (e.g., ChatGPT) for light copyediting (grammar, word choice, and clarity) in portions of the paper. We also used it to assist in checking the recency of citations during the literature review by surfacing potentially relevant recent work. All suggestions were reviewed and verified by the authors; the study design, analyses, claims, and final text are our own.

A.2 Baseline Methods

PPL (Perplexity) Perplexity measures how well the model predicts its own generated answer by aggregating the next-token negative log-likelihood under teacher forcing. For an answer sequence $y_{1:T}$, we define $PPL = \exp\left(-\frac{1}{T} \sum_{t=1}^T \log p_\theta(y_t | y_{<t}, x)\right)$. Larger PPL indicates lower token-level confidence and is often associated with less reliable (and potentially hallucinated) outputs. Because it is computed from a single forward pass on the model’s own answer, PPL is supervision-free and incurs no additional decoding cost.

The teacher-forced log-probability for token position t is gathered from the *previous* timestep’s logits (standard LM shift): $\log p_\theta(y_t | y_{<t}, x) = \log \text{softmax}(L_{t-1})[y_t]$. When scoring an answer window that starts at token index i_1 and ends at i_2 , we therefore use logits on indices $[i_1-1, i_2-1]$ and target tokens on $[i_1, i_2]$; this requires $i_1 > 0$.

Window-Entropy We use an entropy-based uncertainty score over an answer window under teacher forcing. Let $H_t = H(p_\theta(\cdot | y_{<t}, x))$ denote the categorical entropy of the next-token distribution at position t . We operationalize Window-Entropy as a windowed entropy statistic:

$$\text{Win-Ent}_w = \max_{w\text{-window}} \frac{1}{w} \sum_{t \in \text{window}} H_t,$$

and use $w=1$, which reduces to the maximum token entropy over the answer window.

Semantic Entropy Probes (SEP) SEP avoids multi-sample decoding by training a lightweight probe to predict a semantic-uncertainty score (e.g., SE) directly from the model’s internal representations. Concretely, SEP fits a small head (often linear) on top of a selected hidden state (e.g., a fixed position near answer onset) using SE-derived targets. At inference time, SEP is single-pass: extract the hidden state from one forward pass and apply the probe to obtain the score, yielding near-SE discriminative behavior at a cost comparable to other telemetry-based metrics. Because SEP relies on SE targets during training, it is supervision-based even though its test-time computation is cheap.

LLM-Check LLM-Check is a single-pass hallucination detector that fuses token-level uncertainty with representation-based signals extracted from hidden states and attentions under teacher forcing. Specifically, it computes geometric features summarizing the internal trajectory, including mean log-determinant measures of per-layer hidden-state covariance (*Hidden Score*) and attention-kernel maps (*Attention Score*). At inference time LLM-Check is training-free and often improves over uncertainty-only baselines across diverse evaluation settings.

PPL and Window-Entropy are single-pass and training-free. SEP is a training-based but single-pass at inference. LLM-Check is single-pass and training-free (feature computation only).

ICR-probe ICR-probe characterizes *cross-layer residual-stream dynamics* by comparing them to attention-based routing. For token i at layer ℓ , let x_j^ℓ denote the hidden state of token j , let $X^\ell \in \mathbb{R}^{T \times D}$ be the layer hidden-state matrix, and define the residual update as $\Delta x_i^\ell = x_i^\ell - x_i^{\ell-1}$. We induce a distribution over *source* tokens by scoring how well the update aligns with token directions:

$$s_{ij}^\ell \propto \langle \Delta x_i^\ell, x_j^\ell \rangle \quad \Rightarrow \quad \text{Proj}_i^\ell(j) = \frac{\exp(s_{ij}^\ell)}{\sum_k \exp(s_{ik}^\ell)}.$$

Let Attn_i^ℓ be the head-averaged attention distribution for token i at layer ℓ (computed under teacher forcing on the generated answer). ICR then measures the mismatch between where the residual stream is *actually updated* and where attention *allocates* contextual influence: $\text{ICR}_i^\ell = \text{JSD}(\text{Proj}_i^\ell, \text{Attn}_i^\ell)$. To reduce noise and emphasize salient context, we restrict both distributions to

the top- k tokens by attention weight (e.g., $k=20$), and renormalize after truncation.

Pooling and feature construction We compute ICR over answer tokens within an *answer window* W defined by the prompt boundary. For each layer ℓ , we average token-wise scores across $i \in W$ to obtain a layer-level feature: $\mathbf{v} \in \mathbb{R}^L, v_\ell = \frac{1}{|W|} \sum_{i \in W} \text{ICR}_i^\ell$. Larger values of v_ℓ indicate greater divergence between residual updates and attention-based routing, consistent with increased “parametric injection” that is not accounted for by attention-mediated context reuse. We use a small MLP to map the layer-wise feature vector to a sequence-level hallucination probability.

Notes and practicalities

- **Top- k restriction.** Truncating both distributions to the top- k tokens by attention weight suppresses long-tail noise and improves numerical stability.
- **Answer window.** Aggregating over an identified answer span reduces prompt-induced artifacts and targets model-generated content.
- **Access requirements.** ICR-probe assumes white-box (or instrumented) access to hidden states and attention matrices; it does not rely on additional sampling or external retrieval.

B Ablation Studies

We next study which parts of the CORVUS objective contribute most to evasion. We focus on representative training-free single-pass methods (i.e., PPL, Window-Entropy, and LLM-Check components) because they cover the telemetry families targeted by CORVUS. Unless otherwise noted, we report ΔAUROC (attack minus clean, so more negative values indicate stronger evasion) on *FAVA-Annotation*. A representative setting uses Llama-2-7B-Chat with LoRA rank $r=64$, scaling $\alpha=128$, attention/hidden layer band 50–75% of layers, $\lambda_{\text{adv}}=0.5$, $(\beta_{\text{te}}, \beta_{\text{hv}})=(0.07, 0.05)$, and FGSM step size $\varepsilon=1.0 \times 10^{-2}$.

B.1 Per-term Ablation

We ablate the telemetry-shaping terms in the CORVUS objective to identify which signals are responsible for evading LLM-Check. Concretely, we train CORVUS variants that keep only selected subsets of $\{\text{TE}_{\text{clean}}, \overline{\text{HV}}_{\text{clean}}, \overline{\text{AD}}_{\text{adv}}\}$ from Eq. 7,

Baseline	All	HV+AD	TE+AD	TE+HV	TE only	HV only	AD only
PPL (AUROC)	53.18	Δ -5.10	Δ -3.69	Δ -0.61	Δ -4.10	Δ -1.74	Δ -4.58
PPL (ACC)	58.68	Δ -7.78	Δ -8.08	Δ -8.68	Δ -7.78	Δ -8.68	Δ -8.08
Window-Entropy (AUROC)	56.99	Δ -1.69	Δ -5.35	Δ +7.24	Δ -4.20	Δ +0.95	Δ +4.61
Window-Entropy (ACC)	57.19	Δ -8.69	Δ -7.78	Δ -7.19	Δ -2.40	Δ -6.89	Δ -0.90
Hidden L17 (AUROC)	58.15	Δ -4.04	Δ -1.67	Δ +0.39	Δ -2.48	Δ +0.65	Δ -2.38
Hidden L17 (ACC)	56.89	Δ -6.89	Δ -6.89	Δ -2.69	Δ -6.89	Δ -1.80	Δ -6.89
Attn L20 (AUROC)	73.63	Δ -25.54	Δ -19.63	Δ -19.11	Δ -22.80	Δ -2.59	Δ -22.27
Attn L20 (ACC)	69.76	Δ -19.76	Δ -19.76	Δ -19.76	Δ -5.39	Δ -19.76	Δ -19.76

Table 3: **Training-free single-pass detector scores under term ablations on FAVA-Annotation (Llama-2).** The first column shows the original baseline scores; subsequent columns show deltas (Δ = adapted – clean) for CORVUS variants trained with the indicated telemetry terms enabled in Eq. 7 (others set to zero; \mathcal{L}_{CE} always included). AUROC and ACC are measured at the clean-calibrated threshold.

Baseline	No FGSM	$\varepsilon=1.5 \times 10^{-3}$	$\varepsilon=5 \times 10^{-3}$	$(\varepsilon=1.0 \times 10^{-2}, \text{CORVUS})$
PPL (AUROC)	53.18	Δ -4.10	Δ -1.73	Δ -3.85
PPL (ACC)	58.68	Δ -7.78	Δ -8.38	Δ -7.78
Window-Entropy (AUROC)	56.99	Δ -4.20	Δ +1.18	Δ +2.25
Window-Entropy (ACC)	57.19	Δ -2.40	Δ -7.49	Δ -7.78
Hidden L17 (AUROC)	58.15	Δ -2.48	Δ -2.46	Δ -3.18
Hidden L17 (ACC)	56.89	Δ -6.89	Δ -6.89	Δ -6.89
Attn L20 (AUROC)	73.63	Δ -14.80	Δ -16.80	Δ -19.50
Attn L20 (ACC)	69.76	Δ -19.76	Δ -19.76	Δ -19.76

Table 4: **FGSM sweep on FAVA-Annotation (Baseline).** Effect of the embedding-step size ε on Δ AUROC/ Δ ACC (attack – clean) for an LLM-Check detector evaluated on paraphrased prompts. Columns report deltas at $\varepsilon=0$ (no FGSM), 1.5×10^{-3} , 5×10^{-3} , and the default 1.0×10^{-2} of CORVUS.

while holding all other training details fixed. Column headers in Table 3 indicate which of these telemetry-shaping terms are enabled (others set to zero; \mathcal{L}_{CE} is always included). Thus, *AD only* keeps only \overline{AD}_{adv} , while *TE+HV* corresponds to removing the AD term. We then evaluate LLM-Check on FAVA-Annotation and report the change in AUROC. Recall that \overline{AD}_{adv} is applied only on the adversarial (FGSM) pass and encourages higher attention diagonality.

Table 3 shows a clear separation of roles across terms. First, the attention-diagonality term is the most effective single contributor for degrading the attention-based component of LLM-Check: using \overline{AD}_{adv} alone produces the largest AUROC drop for the attention score, and adding it to other terms generally strengthens attention-score evasion. Second, the hidden log-volume term exhibits more mixed behavior under an AUROC lens: it can meaningfully shift hidden-state telemetry (and can worsen fixed operating points), but its effect on ranking performance is not uniformly dominant across components. Third, token-entropy suppression by itself provides only a small change in evasion, and its effect is detector-component dependent; empirically, it behaves more like a complementary knob than a

primary mechanism.

Overall, these results suggest that CORVUS does not rely on a single monolithic failure mode of LLM-Check. Instead, \overline{AD}_{adv} is the main lever for evading attention-centric features, while TE_{clean} and \overline{HV}_{clean} provide secondary shaping that can further perturb uncertainty- and representation-based telemetry depending on the component and operating point.

B.2 Role of the AD-targeted perturbation

This ablation isolates the effect of the AD-targeted FGSM pass. The adversarial perturbation is designed to maximize the surrogate detector score $-AD$ (equivalently, to minimize attention diagonality), producing a proxy pass whose resulting AD_{adv} supplies an additional attention-shaping signal during clean-only training. To quantify its contribution, the embedding-space step size ε is varied and detectors are evaluated on FAVA-Annotation, including paraphrased prompts as a stress test.

As shown in Table 4, removing the adversarial pass ($\varepsilon=0$) consistently reduces evasion under paraphrases, indicating that the AD-targeted proxy pass strengthens the learned attention-telemetry shift beyond what the clean pass alone provides.

Score	AUROC	FPR	TPR@5%FPR	F1
PPL	48.09	2.40	6.59	12.09
Window-Entropy	55.30	4.79	2.99	5.56
Hidden (L17)	54.10	4.19	10.78	18.75
Attn (L20)	48.08	2.99	1.80	3.43

Table 5: **Attack-calibrated operating point at $\varepsilon=1.0\times 10^{-2}$.** Thresholds are selected on attacked telemetry to achieve $\leq 5\%$ FPR (discrete thresholds can yield $\text{FPR} < 5\%$), then TPR@5%FPR and F1 are reported at that threshold. Metrics use the same balanced FAVA-Annotation subset as the other tables.

For nonzero steps, the most effective ε depends on which telemetry family dominates a detector: smaller-to-moderate steps (e.g., $\varepsilon \approx 1.5\times 10^{-3}$) most strongly degrade uncertainty/entropy-driven signals, while larger steps can further amplify degradation of attention-based telemetry. The main experiments therefore use a moderate default that yields strong paraphrase transfer without overly emphasizing a single telemetry component.

Attack-calibrated operating point (oracle). Fixed-threshold deltas (calibrated on the clean model and held fixed) reflect both (i) calibration shift and (ii) changes in ranking separability. To disentangle these, we additionally report an *attack-calibrated* operating point that *reselects* the threshold on attacked telemetry to achieve a target false-positive rate, providing an oracle upper bound on what an auditor could recover if re-calibration were allowed after model-side adaptation. Table 5 reports this attack-calibrated operating point for $\varepsilon=1.0\times 10^{-2}$, including TPR@5%FPR and F1. Notably, the attention score remains near chance even after re-calibration, consistent with a separability collapse rather than a pure threshold shift.

Takeaways. The ablations suggest three points: (i) AD shaping is a primary driver of evasion for attention-centric LLM-Check features; (ii) TE and HV provide complementary shaping signals whose impact varies by detector component and operating point; and (iii) the AD-targeted FGSM pass acts as a telemetry-directed proxy signal that improves paraphrase transfer of the induced internal-signal shift, rather than robustness training or a requirement for in-distribution evasion.